

# Nanoscale

Accepted Manuscript



This is an *Accepted Manuscript*, which has been through the Royal Society of Chemistry peer review process and has been accepted for publication.

*Accepted Manuscripts* are published online shortly after acceptance, before technical editing, formatting and proof reading. Using this free service, authors can make their results available to the community, in citable form, before we publish the edited article. We will replace this *Accepted Manuscript* with the edited and formatted *Advance Article* as soon as it is available.

You can find more information about *Accepted Manuscripts* in the [Information for Authors](#).

Please note that technical editing may introduce minor changes to the text and/or graphics, which may alter content. The journal's standard [Terms & Conditions](#) and the [Ethical guidelines](#) still apply. In no event shall the Royal Society of Chemistry be held responsible for any errors or omissions in this *Accepted Manuscript* or any consequences arising from the use of any information it contains.



Journal Name

ARTICLE

Received 00th January 20xx,  
Accepted 00th January 20xx

DOI: 10.1039/x0xx00000x

www.rsc.org/

## Study of the interactions between endolysin and bacterial peptidoglycan on *S. aureus* by dynamic force spectroscopy

Jianli Liu,<sup>a</sup> Xuejie Zhang,<sup>a</sup> Hang Yang<sup>b</sup>, Jinghe Yuan,<sup>a</sup>  
Hongping Wei<sup>b</sup>, Junping Yu<sup>b\*</sup> and Xiaohong Fang<sup>a\*</sup>

The cell wall binding domain (CBD) of bacteriophage lysins can recognize target bacteria with extraordinary specificity through binding to the bacterial peptidoglycan, thus it is a promising new probe to identify the corresponding bacterial pathogen. In this work, we used atomic force microscopy (AFM) based single-molecule force spectroscopy to investigate the interaction between the CBD of lysin PlyV12 (PlyV12C) and pathogenic bacterium *Staphylococcus aureus* (*S. aureus*). The binding forces of PlyV12C with *S. aureus* have been measured, and the dissociation process of their binding complex has been characterized. Furthermore, we compared the interactions of PlyV12C-*S. aureus* and antibody-*S. aureus*. It is revealed that PlyV12C has a comparable affinity to bacterial peptidoglycans as that of the *S. aureus* antibody. The results provide new information on the binding property of lysin CBD with bacterium, and the application of lysin CBD in bacterium detection.

### Introduction

*Staphylococcus aureus* (*S. aureus*) is Gram-positive bacteria frequently found in skin and nose flora. It is an opportunistic pathogen responsible for many infections such as sepsis, pneumonia, meningitis, endocarditis and osteomyelitis, etc<sup>1,2</sup>. Thus, detection of *S. aureus* is very important. Although antibodies are currently used for the detection of *S. aureus* as well as other bacteria<sup>3,4</sup>, their disadvantages include tedious production, high cost and poor stability. New recognition probes are demanded to detect pathogenic bacteria<sup>5,6</sup>, among which phage lysins have been gaining increasing attention in recent years<sup>6-8</sup>. Phage lysins are a class of bacterium cell wall peptidoglycan hydrolases which are synthesized at the late stage of the bacteriophage lytic cycle to mediate the lysis of host bacterium<sup>9</sup>. The structure of lysins

<sup>a</sup> Beijing National Lab. for Molecular Sciences, Key Laboratory of Molecular Nanostructures and Nanotechnology, Institute of Chemistry, Chinese Academy of Sciences, Beijing 100190, P.R. China

<sup>b</sup> Key Laboratory of Special Pathogens and Biosafety, Wuhan, Institute of Virology, Chinese Academy of Sciences, Wuhan 430071, P.R. China

\* Footnotes relating to the title and/or authors should appear here. Electronic Supplementary Information (ESI) available: [details of any supplementary information available should be included here]. See DOI: 10.1039/x0xx00000x

generally contains two modular domains: N-terminal catalytic domain and C-terminal cell wall binding domain (CBD)<sup>9,10</sup>. The N-terminal catalytic domain of lysins is responsible for destroying bacterial cell walls with high and fast enzymatic activity, whereas the lysins CBD exhibits high specificity towards the cell walls of the host bacterium *via* non-covalent binding to peptidoglycan<sup>11, 12</sup>. Compared with antibodies, lysin CBDs have small size (~20 kDa or smaller), they can be expressed and purified efficiently and chemically modified easily. More importantly, there are quite abundant (about 10<sup>7</sup> or more) peptidoglycan distributed on the surface of host bacterium for lysins binding<sup>13, 14</sup>. Therefore, as a new class of bacterium probes, lysin CBDs have many advantages over antibodies in detecting host bacteria. In addition, lysins can evolve with the bacteria to effectively deal with the newly emerged resistance of bacteria strains, and they do not present a potential toxic threat to humans and animals<sup>10</sup>.

As lysin CBDs are promising probes to specifically recognize host bacteria, the interactions between lysin and bacteria have been characterized by several analytical methods, such as fluorescence microscopy<sup>8, 13, 14</sup>, SPR<sup>15</sup> and AFM<sup>16, 17</sup>. For example, fluorescence imaging has been used to visualize the binding of PlyG to *Bacillus anthracis*<sup>13</sup>, and the dissociation constants for PlyL-*B. anthracis* and PlyG -*B. cereus* strains have been obtained respectively by SPR<sup>15</sup>. Atomic force microscopy (AFM) based single-molecule force spectroscopy (SMFS) has been emerged as a unique tool to quantitatively measure the binding strength at the molecular level for the study of a variety of biomolecular interactions *in vitro* and on live cells<sup>18-20</sup>. It can work in physiological solution and minimally disrupt the surface of live bacterium for *in situ* detection. Recently, the binding forces between Acm2 or LysM and their host bacteria have been obtained by AFM based SMFS technique<sup>16, 17</sup>. In those studies, the two lysins are both N-acetylglucosaminases, one of the four main classes of bacterium cell wall peptidoglycan hydrolases. The full length lysins of Acm2 and LysM were used to localize the peptidoglycan on the nonpathogenic bacterium surfaces, and reveal the binding motif. In this work, we aim to perform a comparative study of the binding properties of lysin CBD and antibody for pathogenic bacterium to investigate the value of lysin CBD in bacterium detection. PlyV12, a lysin from the enterococcal bacteriophage  $\phi$ 1, is used in this study. It belongs to amidase, a different peptidoglycan hydrolases<sup>21</sup>, and

has a relatively broad activity to several enterococcal, streptococcal and staphylococcal strains<sup>22</sup>. PlyV12C, the CBD of PlyV12 can be potentially used to recognize these bacterial pathogens including *S. aureus*, as fluorescence microscopy imaging has proved that PlyV12C binds strongly to *S. aureus*<sup>14</sup>. The results in this study would help to achieve a better understanding of the binding properties of lysin CBD to *S. aureus*, and to explore the potential of lysin CBD in bacterium detection and new bacterium probe screen.

## MATERIALS AND METHODS

### Bacterial strains and growth conditions

The bacterial strain, *S. aureus* (CCTCC, AB9118), was obtained from China Centre for Type Culture Collection (Wuhan, China). *S. aureus* was cultured in Luria-Bertani (LB) broth at 37°C. When bacterium OD 600 arrived at 0.6-0.8, the bacteria were kept in boiling water bath for 15-20 min for inactivation. Then the inactivated bacteria were washed by PBS buffer (137mM NaCl, 2.7mM KCl, 4.3mM Na<sub>2</sub>HPO<sub>4</sub>·H<sub>2</sub>O, 1.4mM KH<sub>2</sub>PO<sub>4</sub>, at pH7.4) twice for AFM experiments.

### PlyV12C expression and purification

The construction of the plasmid pET28a-His<sub>6</sub>-PlyV12C and the expression of the protein PlyV12C were referred to the literature we have published<sup>14</sup>. Briefly, the gene of the bacteriophage endolysin *PlyV12* was synthesized by Songon Biotech Co. (Shanghai, China). The PlyV12C fragment of the gene was obtained by PCR from the *plyV12* gene with the primers PlyV12C-F (5'-GACGG AATTC TTAAC CGGTG GAAGC ACTCC TCCAA AAC-3') and PlyV12C-R (5'-TCGCC TCGAG TTAAT GTACC CCATG CTTC TACC-3'). The plasmid pET28a-His<sub>6</sub>-PlyV12C was confirmed by DNA sequencing. The constructed plasmid was transformed in *E. coli* BL21 (DE3) bacteria for the expression of recombinant protein PlyV12C. After incubating at 37°C until the bacterium OD 600 arrived at 0.4-0.6, the bacteria were induced by isopropyl  $\beta$ -D-thiogalactoside (IPTG) with a final concentration of 1mM at 25°C overnight for PlyV12C expression. Then the bacterial suspensions in binding buffer (20 mM Tris-HCl pH 8.0, 20 mM imidazole, 0.5 M NaCl) were ultrasonicated using an ultrasonication system (Sonic vibra-cell, Ultrasonic processor VCX 750 Watt; Sonics & Materials, Newtown, CT, USA), then centrifuged to eliminate bacteria fragments and

subsequently filtrated by 0.44  $\mu\text{m}$  syringe filter for purification. The protein purification was achieved through a HisTrap<sup>TM</sup>HP column (GE Healthcare) on an AKTA-Prime system (GE Healthcare). Collected fractions were pooled and dialyzed in PBS buffer. After quantitation by the Bradford assay, the purified protein was stored at 4 °C before use.

#### Other reagents

3-Amino-propyltriethoxysilane (APTES), (3-Mercaptopropyl) trimethoxysilane (MPTMS) and peptidoglycan (from *S. aureus*) were purchased from Sigma-Aldrich (USA). The monoclonal antibody of *S. aureus* was obtained from Abcam (London, U.K.). N-hydroxysuccinimide-polyethylene glycol-maleimide (NHS-PEG-MAL, Mw: 3400) was purchased from Laysan Bio (Arab, Alabama, USA). All reagents used in the experiments were of analytical grade except otherwise stated. Milli-Q purified water (18.2 M $\Omega$ ) was used for all experiments.

#### AFM tips preparation

Si<sub>3</sub>N<sub>4</sub> AFM cantilevers (NP-10, Veeco, USA) were used in the experiments. The tips were functionalized with PlyV12C or antibody according to the previously reported procedure<sup>18, 23, 24</sup>. First, the cantilevers were placed in a plasma reactor (ASTP-PJ, USA) to get clean and hydroxylated surfaces. Then the cleaned tips were transferred to a solution of MPTMS (1.0% v/v) in toluene, incubated for 2 h at room temperature for silanization, and then rinsed thoroughly with toluene. The silanized tips were activated by incubation in 1.0 mg/ml NHS-PEG-MAL in dimethylsulfoxide for 3 h, and rinsed thoroughly with dimethylsulfoxide to remove any unbound NHS-PEG-MAL. The activated tips were immersed in the protein solution (10  $\mu\text{g}/\text{ml}$  PlyV12C or antibody in PBS buffer) and incubated at room temperature for 1 h. After rinsing with PBS buffer, the protein-modified tips were stored in PBS buffer at 4 °C until use.

#### Immobilization of *S. aureus*

For AFM measurements, the bacteria were immobilized on silicon wafers by chemical immobilization. According to the previously reported procedures<sup>25</sup>, a single crystal silicon wafer was cut into pieces of approximately 1.5 cm\*1.5 cm before cleaning and modification. The wafers were cleaned and oxidized by heating to

90 °C in piranha solution (7:3 v/v 98% H<sub>2</sub>SO<sub>4</sub>/H<sub>2</sub>O<sub>2</sub>) for 30 min. After washing and drying with high purity nitrogen, the cleaned wafers were immediately transferred to a 5.0% v/v APTES in toluene and incubated for 2 h; afterward, the unbound silanes were washed away by extensive rinsing with toluene. The silanized wafers were activated by incubation in a solution of glutaraldehyde (0.1% v/v) in PBS buffer for 1 h at room temperature and then rinsed with the buffer. 50  $\mu\text{L}$  droplet of *S. aureus* suspension was dispersed on the activated wafers at 4 °C overnight. After silicon wafers were rinsed with PBS buffer, the functionalized substrates were used to experiment.

#### AFM imaging

AFM height and deflection images of the immobilized *S. aureus* were obtained by Bioscope Catalyst AFM (Veeco, Santa Barbara, CA,) in PBS buffer with contact mode at 256 pixels per line, and 0.8Hz scanning rate. Silicon nitride cantilevers (NP-10, Veeco, USA) with a spring constant of 0.06 N/m were used.

#### AFM force measurement

The tip with nominated spring constant 0.06 N/m was used for force measurements. The force measurements between PlyV12C or antibody modified AFM tips and the peptidoglycan or *S. aureus* modified silicon substrate were performed on PicoSPM 5500 (Agilent Technologies, USA) in PBS buffer at room temperature with contact mode. Spring constants of individual cantilevers were calibrated in solution using the thermal noise technique<sup>26</sup>. During the force measurement, the AFM tip engaged at a force of 300 pN, and then retracted at a given pulling velocity. The force-distance curves measured on silicon surface or *S. aureus* were recorded by PicoScan 5 software (Agilent, USA). Dynamic force spectrum experiments were performed at different pulling velocities (ranging from 800 nm/s to 20  $\mu\text{m}/\text{s}$ ) and the loading rates varied from  $8.0 \times 10^2$  pN/s to  $7.0 \times 10^4$  pN/s. Thousands of force-distance curves were collected from different places of silicon surface or 5-6 *S. aureus* cells for each experiment. At each loading rate, at least three independent experiments were performed. The rupture forces between the ligand and receptor were calculated from the retraction curves. Analysis of force-distance curves was completed with a user-defined program in Matlab.

#### RESULTS AND DISCUSSIONS

### Measurement of binding force between PlyV12C and peptidoglycan on silicon wafers

We first measured the binding forces between PlyV12C and peptidoglycan (from *S. aureus*) *in vitro* by AFM-SMFS. For this purpose, we covalently immobilize peptidoglycan onto the silicon substrates and coupled PlyV12C onto the AFM tips *via* a heterobifunctional polyethylene glycol cross-linker. The PEG acted as a spacer to keep PlyV12C flexible for binding and to discriminate nonspecific binding<sup>27</sup>. The low binding probabilities (<30%) are considered to ensure that only one pair of PlyV12C-peptidoglycan formed during the force measurement. After contacting the AFM tip with substrate to form the complex of PlyV12C-peptidoglycan, the tip was then withdrawn from the surface (at the velocity of 1200 nm/s) and a force-distance curve was measured. The representative force curves are presented in Fig. 1A. The rupture peak of PlyV12C-peptidoglycan appears at a certain distance away from the starting point in the force curve, corresponding to the extension of the linker (20–40 nm). When PlyV12C modified AFM tip was blocked by the addition of peptidoglycan solution, the specific peak for PlyV12C-peptidoglycan was hardly detected (as shown in Fig. 1B). The binding probability decreased from  $20.13 \pm 2.79\%$  to  $3.10 \pm 0.88\%$ , confirming that the forces derived from those peaks were the binding forces between PlyV12C and peptidoglycan.

A representative force distribution histogram obtained from 400 to 600 effective force curves is displayed in Fig. 1C. The histogram by Gaussian fitting of one peak supports the measurements of single-molecule forces. The mean value of the most probable single molecular interaction force of PlyV12C and peptidoglycan was determined as  $45.3 \pm 1.4$  pN (from three histograms obtained in three independent experiments).

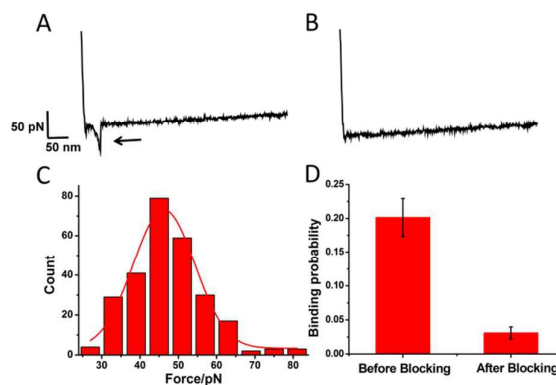


Fig. 1. Interaction forces between PlyV12C and peptidoglycan (from *S. aureus*) on silicon surface probed by AFM-SMFS. (A) A typical force curve obtained between PlyV12C modified AFM tips and peptidoglycan functionalized silicon wafers, of which it reveals a specific binding force of PlyV12C and peptidoglycan. (B) A typical force curve after blocking by peptidoglycan solution, where the typical rupture peak disappeared. (C) Histogram of binding forces between PlyV12C and peptidoglycan (bars, experimental data; solid line, theoretical Gaussian distribution curve). (D) Binding probabilities of PlyV12C to peptidoglycan before and after blocking.

### Immobilization of *S. aureus*

We then tried to carry out the force measurements directly on *S. aureus*. To achieve this goal, the bacteria are immobilized on substrate. Various immobilization approaches have been reported for bacterial cells, such as physical confinement of cells in porous polycarbonate membranes, electrostatic adsorption to positively charged surfaces, and covalently binding to amine- or carboxyl-functionalized surfaces by EDC-NHS chemistry or polyphenolic proteins<sup>25</sup>. In previous AFM force measurements, the bacteria cells were confined on porous polycarbonate membranes<sup>16</sup>. Here, we applied covalent binding method to *S. aureus* immobilization. Immobilization by covalent binding is strong enough to avoid the detachment of bacterium during the force measurements. As shown in Fig. 3, both AFM height (Fig. 2A) and deflection (Fig. 2B) images indicated *S. aureus* cells were well immobilized on silicon surfaces and the density was suitable for force measurements.

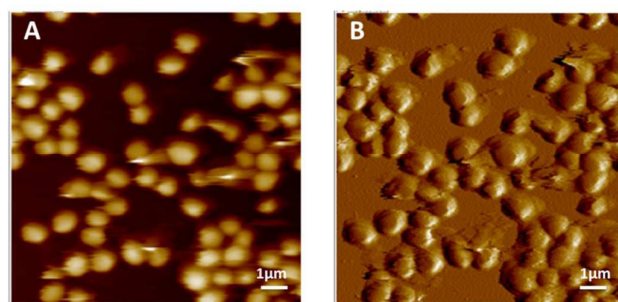


Fig. 2. AFM height (A) and deflection (B) images of *S. aureus* covalently immobilized on the silicon substrate.

### Measurement of binding force between PlyV12C and peptidoglycan on *S. aureus in situ*

After bacteria immobilization, we investigated the interaction forces between the PlyV12C modified AFM tip and peptidoglycan on *S. aureus* cells, where peptidoglycan exists under native conditions. Force measurements were performed using the same conditions as those with the peptidoglycan modified silicon wafers (at the tip velocity of 4000 nm/s). Typical force curve is shown in Fig. 3A and the specific PlyV12C-*S. aureus* interaction forces were obtained, which were confirmed by the blocking experiment (Fig. 3B). Notably, as the bacterial surface was softer than the silicon surface, a less steep slope of force curve on *S. aureus* was observed. After the peptidoglycan solution was added, the binding probability of PlyV12C-peptidoglycan interaction decreased markedly from  $14.63 \pm 2.06\%$  to  $3.40 \pm 1.14\%$  as shown in Fig. 3C, which demonstrated the measurement of specific binding. The single molecular unbinding force of PlyV12C-peptidoglycan was determined as  $52.3 \pm 2.0$  pN. The force of PlyV12C-peptidoglycan measured on *S. aureus in situ* was slightly larger than that on the silicon substrate at the same loading rate, probably due to the

different conformations of peptidoglycans *in vitro* and on bacteria cell walls.

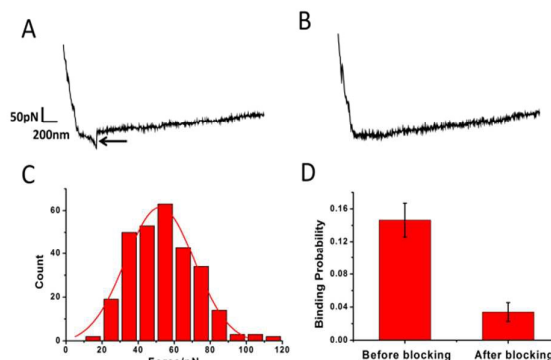


Fig. 3. Interaction forces between PlyV12C and peptidoglycan on *S. aureus* cells probed by AFM SMFS. (A) A typical force curve obtained with PlyV12C-modified AFM tips on *S. aureus*. (B) A typical force curve after the system was blocked with the peptidoglycan solution. (C) A representative histogram of binding forces between PlyV12C and peptidoglycan on *S. aureus* at a pulling speed of 4000 nm/s (bars, experimental data; solid line, theoretical Gaussian distribution curve). (D) Binding probabilities of PlyV12C to peptidoglycan on *S. aureus* before and after blocking with free peptidoglycan molecules.

### Measurement of binding force between antibody and *S. aureus*

To check whether PlyV12C has a strong binding strength to *S. aureus* that rivals antibody, we changed the AFM tips to those modified with the antibody and performed force measurements as described above at the same tip velocity (4000 nm/s). From the histogram of the force distribution, the most probable rupture force between antibody and *S. aureus* was fitted as  $56.7 \pm 0.9$  pN (Fig.

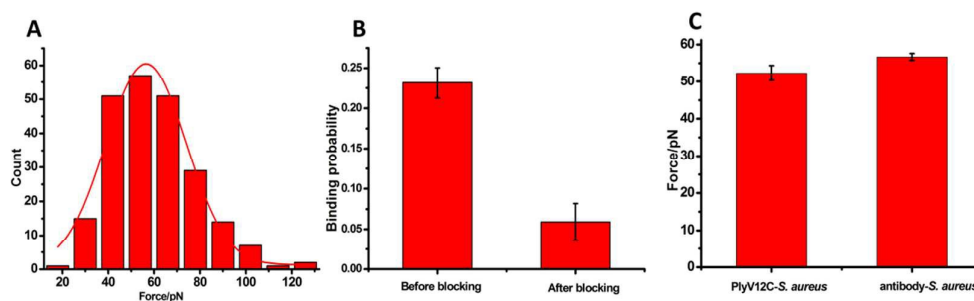


Fig. 4. Interaction forces between antibody and *S. aureus* cells probed by AFM-SMFS. (A) Histogram of binding forces of antibody-*S. aureus* at a pulling speed of 4000nm/s (bars, experimental data; solid line, theoretical Gaussian distribution curve). (B) Binding probabilities of antibody to *S. aureus* before and after blocking with antibody solution. (C) The comparison of binding forces of PlyV12C-*S. aureus* and antibody-*S. aureus* at the same loading rate.

4A). Control experiments were also performed to confirm their specific interaction, and the corresponding binding probability was decreased obviously in control (from 23.17±1.89% to 5.90±2.29%, Fig. 4B). The interaction forces of PlyV12C-*S. aureus* (52.3±2.0 pN) and antibody-*S. aureus* (56.7±0.9 pN) are quite close (Fig. 4C), indicating the comparable affinities of PlyV12C and antibody toward *S. aureus*.

#### Dynamic force spectra of PlyV12C-*S. aureus* and antibody-*S. aureus*

It is known that the binding force ( $F$ ) between a pair of receptor-ligand measured by SMFS depends on the applied AFM loading rate ( $r$ ). According to Bell model, their relationship can be described by the following equation<sup>28, 29</sup>:

$$F = \frac{k_B T}{x_\beta} * \ln\left(\frac{r \chi_\beta}{k_{off}(0) k_B T}\right)$$

where  $k_B$  is the Boltzman constant,  $T$  is the absolute temperature,  $F$  is the most probable unbinding force,  $k_{off}(0)$  is the dissociation rate constant at zero applied force,  $\chi_\beta$  is the distance of the energy barrier of the dissociated state to bound state, and  $r$  is the loading rate, which was calculated using the slope of the force peak times the pulling velocity and then times the spring constant of the AFM tip.

Therefore, by measuring the forces at different loading rates and plotting the dynamic force spectra, more information on the ligand-receptor dissociation kinetic parameters can be derived. We further carried out the comparative study of the dissociation properties of PlyV12C-*S. aureus* and antibody-*S. aureus* by dynamic force spectra (DFS). The plots of the unbinding forces versus loading rates are displayed in Fig. 5. The data revealed that the rupture force values of antibody-*S. aureus* were always slightly larger than those of PlyV12C-*S. aureus* under the same loading rates. Interestingly, the dynamic force spectra of PlyV12C-*S. aureus* and antibody-*S. aureus* both show two linear regimes, indicating the dissociation of these two complexes went through two energy

barriers from association state to dissociation state. The dissociation rate constant  $k_{off}$  and the distance between dissociation and bound status ( $\chi_\beta$ ) were calculated from the slope and intercept of the  $F$ - $\ln r$  plot. The linear regime at the low loading rate mapped the outer barriers<sup>30</sup>. In this section, the values of  $k_{off}$  and  $\chi_\beta$  for PlyV12C-*S. aureus* and antibody-*S. aureus* interactions were calculated as  $\chi_\beta$  (PlyV12C) = 0.36 nm,  $k_{off}$  (PlyV12C) = 9.57s<sup>-1</sup> and  $\chi_\beta$  (antibody) = 0.37 nm,  $k_{off}$  (antibody) = 4.63 s<sup>-1</sup>, respectively. The linear regime at the high loading rate governed the inner barriers. In that section, the values of  $k_{off}$  and  $\chi_\beta$  for PlyV12C-*S. aureus* and antibody-*S. aureus* were derived as  $\chi_\beta$  (PlyV12C) = 0.13 nm,  $k_{off}$  (PlyV12C) = 68.1 s<sup>-1</sup> and  $\chi_\beta$  (antibody) = 0.14 nm,  $k_{off}$  (antibody) = 41.6 s<sup>-1</sup>, respectively.

Compared with previous reports about lysin-peptidoglycan interaction<sup>16, 17</sup>, the DFS spectra of LysM-peptidoglycan and Acm2-peptidoglycan binding were fitted by only one linear regime. Besides, the kinetic parameter  $k_{off}$  is one order of magnitude smaller than values obtained in our study. The possible reasons might be the binding properties involved between different lysin-peptidoglycan themselves. In addition, unlike LysM and Acm2 which are the full length lysins, PlyV12C is lack of N-terminal catalytic domain. In our study, the kinetic parameters of the interactions between PlyV12C and *S. aureus* are close to those of antibody-*S. aureus*, demonstrating that the affinity of PlyV12C to *S. aureus* is quite similar to that of antibody to *S. aureus*, both of which are considerably stable.

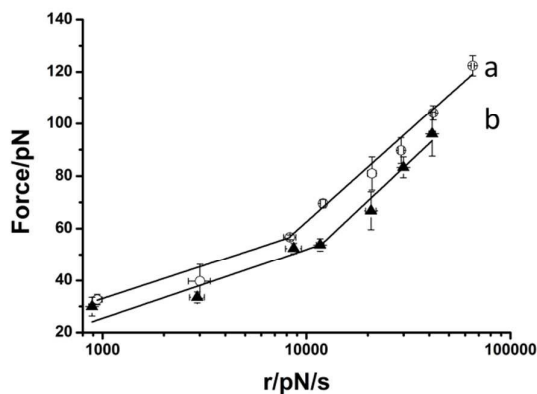


Fig. 5. Comparison of dynamic force spectra of antibody-*S. aureus*(a) and PlyV12C-*S. aureus*(b). For forces measured at different loading rates for antibody-*S. aureus* and PlyV12C-*S. aureus*, there were two linear regions. At each loading rate, the data were shown as the mean values and standard error of the results from at least three independent experiments.

## Conclusions

In summary, the quantitative binding forces of PlyV12C-peptidoglycan, PlyV12C-*S. aureus* and antibody-*S. aureus* as well as the dynamic force spectra were obtained by AFM-SMFS. For the first time, we compared the dissociation processes of PlyV12C-peptidoglycan complex with that of antibody-*S. aureus*. The results demonstrated these two complexes both experience intermediate states and overcome two activation barriers to dissociation states with similar dissociation rate constants. The study supports that the lysine CBD, PlyV12C, is a high-affinity probe for the detection of *S. aureus*.

## Acknowledgements

This work was supported by the financial support of the National Basic Research Program of China (2013CB933701), and National Natural Science Foundation of China (Nos. 21105114, 21121063).

## References

- 1 P. Szweda, M. Schielmann, R. Kotlowski, G. Gorczyca, M. Zalewska and S. Milewski, *Applied microbiology and biotechnology*, 2012, 96, 1157-1174.

- 2 D. B. Gilmer, J. E. Schmitz, C. W. Euler and V. A. Fischetti, *Antimicrobial agents and chemotherapy*, 2013, 57, 2743-2750.
- 3 E. R. Goldman, G. P. Anderson, J. L. Liu, J. B. Delehanty, L. J. Sherwood, L. E. Osborn, L. B. Cummins and A. Hayhurst, *Analytical chemistry*, 2006, 78, 8245-8255.
- 4 N. Ertas, Z. Gonulalan, Y. Yildirim and E. Kum, *International Journal of Food Microbiology*, 2010, 142, 74-77.
- 5 S. S. Rao, K. V. K. Mohan, Y. Gao and C. D. Atreya, *Microbiological Research*, 2013, 168, 106-112.
- 6 M. Tolba, M. U. Ahmed, C. Tlili, F. Eichenseher, M. J. Loessner and M. Zourab, *The Analyst*, 2012, 137, 5749-5756.
- 7 S. Sainathrao, K. V. K. Mohan and C. Atreya, *Bmc Biotechnology*, 2009, 9.
- 8 M. Schmelcher, T. Shabarova, M. R. Eugster, F. Eichenseher, V. S. Tchang, M. Banz and M. J. Loessner, *Applied and Environmental Microbiology*, 2010, 76, 5745-5756.
- 9 M. Pastagia, R. Schuch, V. A. Fischetti and D. B. Huang, *Journal of medical microbiology*, 2013, 62, 1506-1516.
- 10 J. Borysowski, B. Weber-Dabrowska and A. Gorski, *Experimental Biology and Medicine*, 2006, 231, 366-377.
- 11 M. J. Loessner, K. Kramer, F. Ebel and S. Scherer, *Molecular microbiology*, 2002, 44, 335-349.
- 12 M. J. Loessner, *Current Opinion in Microbiology*, 2005, 8, 480-487.
- 13 H. Yang, D.-B. Wang, Q. Dong, Z. Zhang, Z. Cui, J. Deng, J. Yu, X.-e. Zhang and H. Wei, *Antimicrobial agents and chemotherapy*, 2012, 56, 5031-5039.
- 14 Q. Dong, J. Wang, H. Yang, C. Wei, J. Yu, Y. Zhang, Y. Huang, X.-E. Zhang and H. Wei, *Microbial Biotechnology*, 2015, 8, 210-220.
- 15 J. Ganguly, L. Y. Low, N. Kamal, E. Saile, L. S. Forsberg, G. Gutierrez-Sanchez, A. R. Hoffmaster, R. Liddington, C. P. Quinn, R. W. Carlson and E. L. Kannenberg, *Glycobiology*, 2013, 23, 820-832.
- 16 G. Andre, K. Leenhouts, P. Hols and Y. F. Dufrene, *Journal of Bacteriology*, 2008, 190, 7079-7086.
- 17 A. Beaussart, T. Rolain, M.-C. Duchene, S. El-Kirat-Chatel, G. Andre, P. Hols and Y. F. Dufrene, *Biophysical journal*, 2013, 105, 620-629.
- 18 X. Shi, X. Zhang, T. Xia and X. Fang, *Nanomedicine : nanotechnology, biology, and medicine*, 2012, 7, 1625-1637.
- 19 W. Zhao, M. Cai, H. Xu, J. Jiang and H. Wang, *Nanoscale*, 2013, 5, 3226-3229.
- 20 M. B. O'Donoghue, X. Shi, X. Fang and W. Tan, *Analytical and bioanalytical chemistry*, 2012, 402, 3205-3209.
- 21 P. Yoong, R. Schuch, D. Nelson and V. A. Fischetti, *Journal of Bacteriology*, 2004, 186, 4808-4812.

## ARTICLE

Journal Name

- 22 P. Yoong, R. Schuch, D. Nelson and V. A. Fischetti, *J Bacteriol*, 2004, 186, 4808-4812.
- 23 J. Yu, Q. Wang, X. Shi, X. Ma, H. Yang, Y.-G. Chen and X. Fang, *Journal of Physical Chemistry B*, 2007, 111, 13619-13625.
- 24 X. Zhang, X. Shi, L. Xu, J. Yuan and X. Fang, *Nanomedicine-Nanotechnology Biology and Medicine*, 2013, 9, 627-635.
- 25 R. Louise Meyer, X. Zhou, L. Tang, A. Arpanaei, P. Kingshott and F. Besenbacher, *Ultramicroscopy*, 2010, 110, 1349-1357.
- 26 J. L. Hutter and J. Bechhoefer, *Review of Scientific Instruments*, 1993, 64, 3342-3342.
- 27 F. Kienberger, A. Ebner, H. J. Gruber and P. Hinterdorfer, *Accounts of Chemical Research*, 2006, 39, 29-36.
- 28 G. I. Bell, *Science*, 1978, 200, 618-627.
- 29 E. Evans and K. Ritchie, *Biophysical journal*, 1997, 72, 1541-1555.
- 30 L. Ge, G. Jin and X. Fang, *Langmuir : the ACS journal of surfaces and colloids*, 2012, 28, 707-713.